Biochimica et Biophysica Acta 1838 (2014) 2216–2227

Contents lists available at ScienceDirect

Biochimica et Biophysica Acta

journal homepage: www.elsevier.com/locate/bbamem

Review

Membrane-active peptides: Binding, translocation, and flux in lipid vesicles☆

Paulo F. Almeida *

Department of Chemistry and Biochemistry, University of North Carolina Wilmington, Wilmington, NC 28403, USA

ARTICLE INFO

Article history:
Received 3 February 2014
Received in revised form 14 April 2014
Accepted 17 April 2014
Available online 25 April 2014

Keywords:
Antimicrobial
Cell-penetrating
Amphipathic
Binding
Translocation
Hydrophobicity

ABSTRACT

Recently, new and improved methods have been developed to measure translocation of membrane-active peptides (antimicrobial, cytolytic, and amphipathic cell-penetrating peptides) across lipid bilayer membranes. The hypothesis that translocation of membrane-active peptides across a lipid bilayer is determined by the Gibbs energy of insertion of the peptide into the bilayer is re-examined in the light of new experimental tests. The original hypothesis and its motivation are first revisited, examining some of the specific predictions that it generated, followed by the results of the initial tests. Translocation is understood as requiring two previous steps: binding and insertion in the membrane. The problem of peptide binding to membranes, its prediction, measurement, and calculation are addressed. Particular attention is given to understanding the reason for the need for amphipathic structures in the function of membrane-active peptides. Insertion into the membrane is then examined. Hydrophobicity scales are compared, and their influence on calculations is discussed. The relation between translocation and graded or all-or-none peptide-induced flux from or into lipid vesicles is also considered. Finally, the most recent work on translocation is examined, both experimental and from molecular dynamics simulations. This article is part of a Special Issue entitled: Interfacially Active Peptides and Proteins. Guest Editors: William C. Wimley and Kalina Hristova.

Contents

1. Introduction

Five years ago, we proposed the hypothesis that translocation of membrane-active peptides (antimicrobial, cytolytic, and amphipathic cell-penetrating peptides) across a lipid bilayer is determined by the Gibbs energy of insertion of the peptide into the bilayer [1]. In that article we emphasized the broad similarities of the structures and the activity of

☆ This article is part of a Special Issue entitled: Interfacially Active Peptides and Proteins. Guest Editors: William C. Wimley and Kalina Hristova.

* Tel.: +1 910 962 7300; fax: +1 910 962 3013.
E-mail address: almeidap@uncw.edu.

http://dx.doi.org/10.1016/j.bbamem.2014.04.014
0005-2736/

those various peptides. We further suggested that these peptides are not fundamentally distinct, but differ only quantitatively in the weight the various structural properties contribute to their overall function.

Now I re-examine that hypothesis in the light of experimental tests performed since then, concentrating especially on the question of peptide translocation. Recent experiments from other groups [2,3] and our own laboratory [4] have provided new breakthroughs in the investigation of peptide translocation across membranes. This progress is due in great measure to the development of several new and improved methods to measure translocation [2–4], an experiment that has proved difficult and elusive.

I will begin by restating the original hypothesis and its motivation, examining some of the specific predictions it generated, and the results of initial tests. Then, the problem of peptide binding to membranes, its prediction, measurement, and calculation is addressed in some detail. Particular attention is devoted to understand the reason for the need for amphipathic structures in the function of membrane-active peptides. Intuition appears to be misleading in this matter. The next step in the mechanism of these peptides—insertion into the membrane—is then examined. Hydrophobicity scales are compared, and their influence on calculations is discussed. Finally, I consider translocation. Recent work, both experimental and using molecular dynamics (MD) simulations, on the relation between translocation and graded or all-or-none peptide-induced dye flux in lipid vesicles, is also reviewed.

2. Hypothesis

The hypothesis we proposed is that peptide translocation across a membrane is determined by the Gibbs energy of insertion (ΔG^o_{ins}) into the bilayer [1]. To understand the idea, consider the diagram of Fig. 1, which shows the interaction of a membrane-active peptide with a lipid bilayer. The peptide, initially in water, binds to the membrane with a Gibbs energy of binding ΔG^o_{bind}. The state of the peptide associated with the membrane interface (*if*) is the most stable. From here, the peptide can insert into the membrane with ΔG^o_{ins}. Because this step leads to an unfavorable state it should determine, in the main, the rate of the overall translocation process. According to the classic postulate of Hammond [5], this unstable intermediate should in fact resemble the transition state in the kinetic mechanism of translocation. Therefore, we should have $\Delta G^o_{ins} \approx \Delta G^{\ddagger}$, the free energy of the transition state. On purpose, in the original [6] and subsequent articles, we represented this membrane-inserted state in an unrealistic manner, with the peptide inside the membrane, oriented parallel to the surface (Fig. 1). This cartoon was not meant to depict the structure of the inserted state, but only to represent the thermodynamic cycle. No mechanism of insertion was, or is, implied. Indeed, it is generally believed that an orientation of the peptide almost perpendicular to the bilayer surface is more realistic. But this unstable intermediate is not accessible experimentally by any available technique. Molecular dynamics (MD) simulations offer a glimpse of what it may look like, and in most cases the peptides are not parallel to the membrane, but oblique or perpendicular [7–11].

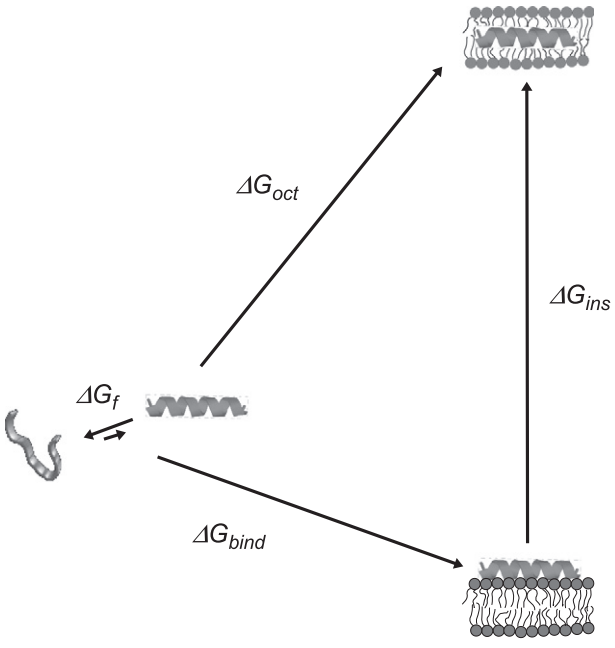

Fig. 1. Thermodynamic cycle for the interactions of a membrane-active peptide with a membrane. Peptide in water (left) and on the membrane interface (bottom right) or inserted in the bilayer (top right). No information on orientation is implied. The Gibbs energies in each step are: ΔG_{bind}, binding to the lipid bilayer interface; ΔG_{oct}, insertion into the bilayer core, approximated by the Gibbs energy of transfer to octanol; $\Delta G_{ins} = \Delta G_{oct} - \Delta G_{bind}$, insertion into the bilayer interior; and ΔG_f, folding in water.
Modified from Yandek et al. [6], Biophys. J. 92, 2434–2444. Copyright (2007) Elsevier.

To have predictive value, the hypothesis needs to allow calculation of ΔG^o_{ins}. The Gibbs energy of the peptide state associated with the membrane interface relative to water can be measured by determining the binding equilibrium constant. But since the inserted state is not experimentally accessible, its Gibbs energy can only be calculated. To that end, we have used the Gibbs energy of transfer of the peptide from water to octanol (ΔG^o_{oct}), obtained from the Wimley–White octanol hydrophobicity scale [12,13]. Even though the bilayer interior is not similar to octanol, this scale has proved excellent in predicting the transmembrane segments of integral proteins [14], which lends confidence to its use in the calculation of Gibbs energy of transfer from water to the bilayer interior. Thus, $\Delta G^o_{ins} \approx \Delta G^o_{oct} - \Delta G^o_{bind}$. The contribution of folding in water (ΔG^o_f) will be discussed later, but is usually small. If ΔG^o_{bind} is not available experimentally, it can be calculated from the Wimley–White interfacial hydrophobicity scale [13,15], established for the transfer of peptides from water to the interface of a membrane of pure 1-palmitoyl-2-oleoylphosphatidylcholine (POPC). We then hypothesized that if $\Delta G^o_{ins} \leq 20$ kcal/mol the peptides are able to translocate across the lipid bilayer, but if $\Delta G^o_{ins} > 23$ kcal/mol they cannot [1]. A "gray zone" may exist for ΔG^o_{ins} between about 20–23 kcal/mol, in which either mechanism may prevail. What is the basis for this threshold?

We have measured the kinetics of dye efflux induced by a series of amphipathic peptides, representative of the antimicrobial, cell-penetrating peptides, and cytolytic types. Those data were analyzed with rigorous kinetic mechanisms, derived from the numerical solution of the differential rate equations [6,16–20]. In several cases, to fit the integrated rate equations to the experimental data we needed to postulate translocation of the peptide across the membrane [6,18–20]. This proved necessary to account for the incomplete dye release observed in those cases, even at very long times. The physical mechanism to justify this assumption is that dye flux occurs while the membrane is perturbed, and the membrane is perturbed by interaction with the peptide while a mass imbalance of the peptide exists across the bilayer. But if the peptide is able to translocate, it eventually equilibrates across the membrane, and becomes about evenly distributed across the bilayer. The perturbation then disappears and efflux stops. When this kind of behavior was observed translocation was postulated. In those cases, we further assumed that dye efflux occurred concomitant with peptide translocation. This second assumption now appears not to be correct. We will return to this topic at the end. Some other peptides, namely magainin 2 and cecropin A, caused a slow but complete release, and there was no kinetic evidence for translocation [16,17]. Those peptides were thought to function by a different mechanism: the stress resulting from peptide accumulation on the surface of the outer leaflet of the bilayer eventually induced a larger response from the membrane, which included formation of transient pores.

Upon interaction with a peptide, a lipid vesicle can release its contents in two extreme ways: graded or all-or-none [1,21]. Graded release (or flux) occurs when, at the midpoint of the dye efflux reaction, most

vesicles contain about one-half of their initial dye content. In all-or-none release, at the midpoint, about half of the vesicles contain almost all of their initial dye, while the other half has released everything. (See Fig. 7, discussed below, for experimentally determined examples of distributions of each type.) Graded and all-or-none release was determined using a fluorescence requenching assay [22–24]. The cases in which translocation was postulated in the analysis of dye efflux kinetics coincided with peptides that induced graded release. Further, we noticed that peptides that caused graded dye release had $\Delta G^o_{ins} \leq 20$ kcal/mol, whereas peptides that caused all-or-none release had $\Delta G^o_{ins} > 23$ kcal/mol. This suggested the following logical relation between the type of release and ΔG^o_{ins}:

$$\Delta G^o_{ins} \leq 20 \text{ kcal/mol} \Rightarrow \quad \text{translocation} \Rightarrow \quad \text{graded release} \tag{1}$$

$$\Delta G^o_{ins} \geq 23 \text{ kcal/mol} \Rightarrow \quad \text{no translocation} \Rightarrow \quad \text{all-or-none release.} \tag{2}$$

The connection between the thermodynamics of insertion and the observed release was thus ascribed to the translocation of the peptide across the membrane. This idea provided a simple explanation for the lack of a clear influence of peptide sequence on their activity. If all that matters is the Gibbs energy of insertion, there are no specific effects of sequence.

In fact, despite countless papers on the subject, the only clear relation between sequence and activity is that cationic amino acid residues are essential for binding to negatively charged membranes, such as those containing phosphatidylglycerol (PG). This explains why most antimicrobial peptides have several basic residues (lysine and arginine), which are essential for interaction with negatively charged bacterial membranes. Conversely, those cationic residues prevent binding to zwitterionic membranes (neutral), typically composed of PC, which are representative of the outer leaflet of the lipid bilayer of eukaryotic membranes, because of their unfavorable Gibbs energy of transfer to the bilayer interface [13,15]; hence, the antimicrobial peptide specificity. But this is little in the way of specificity. Furthermore, the effect of the peptide positive charge is a matter of composition, not sequence. Similarly, peptide hydrophobicity is important for binding, but this is again an effect of composition only. Indeed, paradoxically, peptide amphipathicity, measured by the hydrophobic moment (μ_H), seems to play little or no role in binding, as long as the secondary structure remains constant. What these observations suggest is that the amino acid composition of peptides matters for activity but the detailed sequence, to a large extent, does not. This is easy to understand if the sequence only matters in as much as it determines the thermodynamics of binding and insertion into the membrane. But is this true?

3. Specific predictions

If sequence matters for peptide activity only to the extent that it determines the Gibbs energy changes of binding (ΔG^o_{bind}) and insertion (ΔG^o_{ins}), there is a simple corollary that must be true. It should be possible to replace the sequence of a peptide by a minimalist version, which preserves charge, amphipathicity, hydrophobicity, and helicity (or secondary structure)—and thus preserves the thermodynamic properties—but is otherwise simplified to include only alanine, leucine, and the charged amino acids, plus those residues that may play special roles in structure, such as proline, glycine, and aromatics. This prediction was tested in simplified versions of the antimicrobial peptides magainin 2, cecropin A, TP10W, and δ-lysin [25,26].

Variants of magainin 2 and cecropin A, called MG-2 and CE-2, were designed in which small moderately polar residues were replaced by alanine, and hydrophobic residues, by leucine. The other residues were generally retained, with small adjustments to maintain ΔG^o_{bind}, ΔG^o_{ins}, and μ_H essentially the same as in the original peptides [26]. We found that, as sought, binding and activity were conserved: binding to POPC remained essentially constant in the mutant peptides; and activity, measured by the mean time (τ) of dye efflux induced in POPC vesicles, was also maintained (Table 1). Now, both magainin 2 and cecropin A cause all-or-none dye release [16,17,27]. The same was expected for MG-2 and CE-2, because ΔG^o_{ins} was about the same in the mutants and the original peptides, ~27 kcal/mol in magainin and MG-2, and ~36 kcal/mol in cecropin A and CE-2. In all cases, all-or-none release was expected because $\Delta G^o_{ins} > 23$ kcal/mol. Surprisingly, release changed dramatically to graded in both MG-2 and CE-2 (Fig. 2).

Our idea was that graded release occurred as a consequence of translocation. But clearly, either those peptides are able to translocate across the lipid bilayer despite the large unfavorable values of insertion (ΔG^o_{ins}), or they do not translocate but still cause graded release, by some other mechanism. In fact, release was incomplete with the other graded peptides, but it is complete with CE-2 and MG-2 [26], which is consistent with a constant surface perturbation of the membrane, rather than with a translocation that stops when the peptides equilibrate across the membrane. In any case, either the idea that insertion occurs if ΔG^o_{ins} is lower than a certain threshold is not correct, or graded and all-or-none release are not reliable indicators of translocation or its absence. It became important to determine which one is true.

We also noticed that the Gibbs energy of binding ΔG^o_{if} calculated with the Wimley—White POPC interfacial scale [13,15] was usually in good agreement with the measured ΔG^o_{bind} [1,25] (see Fig. 3 below). However, a significant discrepancy was observed with a few peptides [1,26]. The most blatant cases are those of δ-lysin and cecropin A. Now, when these peptides adopt a helical conformation, several acidic and basic residues are within hydrogen bonding distance of each other. We conjectured that if the side chains of those residues were involved in salt bridges, the additional contribution to the Gibbs energy of binding could account for the discrepancy [1]. Indeed, as pointed out by Wimley et al. [28], the Gibbs energy of binding to the interface arises almost entirely from the acquisition of secondary structure, not from the peptide hydrophobicity. Further, Wimley et al. [29] measured the contribution of side chain salt bridges for partitioning into octanol to be ≈−4 kcal/mol, and suggested that a smaller contribution, probably ≈−0.5 kcal/mol, may apply to transfer to a POPC membrane interface. Since the residue hydrophobicity values in the Wimley–White interfacial and octanol scales vary by a factor of ~2 (see Fig. 6A below), we hypothesized that side chain salt bridges at the interface contribute half the value in octanol, that is, ≈−2 kcal/mol, to the binding energy. Using this value, the calculated ΔG^o_{if} and the measured ΔG^o_{bind} of δ-lysin and cecropin A to POPC membranes could be reconciled. Further, inclusion of putative salt bridges decreased the values of ΔG^o_{ins} for some of those peptides, so that they conformed to the idea that graded release corresponded to $\Delta G^o_{ins} < \sim 20$ kcal/mol.

The prediction that side-chain salt bridges at the interface and inside the membrane lower ΔG^o_{bind} and ΔG^o_{ins} was also tested. Variants of these peptides were designed which either should contain more salt bridges, by replacing acidic with basic residues (or vice-versa) within hydrogen-bonding distance, or should contain fewer (or none), by replacing all acidic residues with basic ones. We found that, contrary to prediction, the introduction or suppression of putative salt bridges did not change ΔG^o_{ins}. Thus, either the attempt to engineer side-chain salt bridges failed, or their contribution to the peptide stability at the interface is small, probably more in line with ≈−0.5 kcal/mol suggested by Wimley et al. [29].

In summary, the two predictions regarding sequence effects, generated from the main hypothesis under the assumption that release type informs on translocation, were found to be wrong in general. Whether or not the main hypothesis itself—that peptide translocation occurs if ΔG^o_{ins} is below a certain threshold ~20 kcal/mol—is correct requires a more careful examination of the steps contributing to insertion ($\Delta G^o_{ins} = \Delta G^o_{oct} - \Delta G^o_{bind}$). In the next sections, the thermodynamics of binding and insertion will be examined in some detail. We will see that determination of the type of release, as graded or all-or-none, is not a

Table 1
Thermodynamic and kinetic data for the peptides discussed.

Peptide (refs.)[a]	N	ΔG^o_{bind}	ΔG^o_{if}	ΔG^o_{oct}	ΔG^o_{ins}	% Helix			μ_H	μ_H/N	k_{on}	k_{off}	K_D	τ[b]
	(res.)	(kcal/mol)				Memb.	Water	Agadir[c]	WW	Interface	(M^{-1} s^{-1})	(s^{-1})	(μM)	(s)
δ-Lysin family														
δ-Lysin [26]	26	−8.5	−5.3	21.9	30.4	100	53	1	7.75	0.30	2.0×10^3	0.06	30	2.2
DL-1 [26]	26	−7.0	−1.3	19.3	26.4	52	20	1	7.18	0.28	2.5×10^4	10	400	4.9
DL-2b [26]	26	−5.7	−5.7	19.7	25.4	77	54	35	8.77	0.34	2.5×10^3	8.6	3400	650
DL-2a [26]	26	−7.4	−1.8	23.2	30.6	54	59	59	7.65	0.29	5.5×10^2	0.11	200	14.8
TP10 family														
TP10W [4,25]	21	−7.7	−7.3	9.3	17.0	57	28	23	3.75	0.18	9.4×10^4	12.7	140	12
TPW-1 [25]	21	−7.0	−6.3	11.0	18.0	50	27	27	4.03	0.19	4.0×10^4	16	400	220
TPW-2 [25]	21	−10.1	−9.5	8.7	18.8	75	38	27	3.91	0.19	1.6×10^5	0.37	2.3	0.7
TPW-3 [25]	21	−7.1	−7.1	10.2	17.3	57	28	28	3.83	0.18	7.8×10^4	25	320	3.8
TP10 [6,65]	21	−6.3	−6.3	10.7	17.0	(55)[d]	(23)	23	3.48	0.17			1300	170
TP10-COO^- [65]	21	−4.5	−4.5	14.3	18.8	(55)	(15)	15	3.48	0.17			29,000	19,000
TP10W-COO^- [65]	21	−7.4	−5.4	12.9	20.3	(55)	(15)	15	3.75	0.18	4.8×10^5	100	210	1650
TP10-7MC[e] [65]	21	−8.8	−9.1	5.8	14.6	(55)	(23)	23	3.03	0.14	7.4×10^4	1.5	20	11
Cecropin family														
Cecropin A [16]	37	−6.4	−1.6	31.1	37.6	63	10	1	4.86	0.13	2.8×10^5	300	1100	15,000
CE-1 [26]	37	−7.0	−5.8	17.3	24.3	55	30	3	7.33	0.20	1.9×10^4	7.5	400	35
CE-2 [26]	37	−5.6	−5.4	29.6	35.2	70	30	4	5.23	0.14	3.0×10^4	138	4600	11,000
Magainin family														
Magainin 2[f] [17,26,35]	23	−6.1	−6.1	20.1	26.1	83	5	0	6.50	0.28	2.5×10^5	500	2000	20,000
MG-1 [26]	23	−7.4	−3.2	18.2	25.6	69	46	16	9.13	0.40	6.1×10^4	12.7	210	13.5
MG-2 [26]	23	−6.4	−5.5	21.3	27.7	80	10	2	7.00	0.30	2.1×10^4	24	1100	20,000
Mastoparan X [20]	14	−7.2	−6.9	8.7	15.9	86	2	2	3.96	0.28	8.6×10^4	24	280	3000
Melittin [1,66–70]	26	−7.6	−7.3	12.0	19.6	70	7	7	5.18	0.20	2.0×10^4	3.1	150	
AQL peptides [33,40]														
A8Q3L4-0.55	17	−5.20	−5.5	2.4	7.6	30	9.2	13	0.55	0.03			8700	
A8Q3L4-2.00	17	−5.70	−5.9	2.4	8.1	36	15.8	14	2.00	0.12			3700	
A8Q3L4-2.86	17	−5.90	−6.5	2.4	8.3	46	21.2	21	2.86	0.17			2700	
A8Q3L4-4.72	17	−6.40	−7.9	2.4	8.8	67	29.2	33	4.72	0.28			1100	
A8Q3L4-5.51	17	−7.30	−8.1	2.4	9.7	72	38	35	5.51	0.32			250	
A8Q3L4-5.54	17	−7.40	−8.2	2.4	9.8	73	39.6	33	5.54	0.33			210	

[a] For sequences, see references for each peptide.
[b] Mean time of carboxyfluorescein efflux induced by 1 μM peptide on 50 μM POPC LUVs.
[c] Refs. [59–64]
[d] Values in parentheses are estimates based on the most similar peptides or on Agadir.
[e] In calculations, Trp was used as a mimic for Lys-7-methoxycoumarin (residue 7) because it yields ΔG^o_{if} most similar to ΔG^o_{bind}.
[f] Some data are for the F12W variant, which behaves similarly to the original; see references cited.

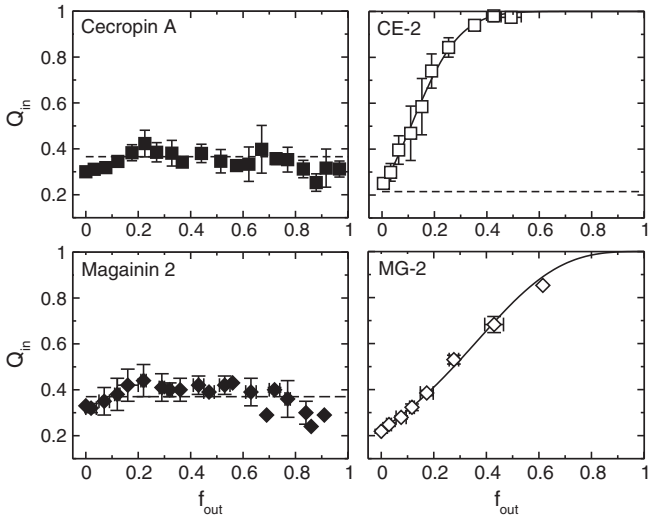

Fig. 2. Fluorescence requenching assay. Left, the original peptides, cecropin A [16] and magainin 2 [17]. Right, their variants CE-2 and MG-2 [26]. Q_{in}, fluorescence quenching factor inside the vesicles is plotted against the fraction of fluorophore released, f_{out}. All-or-none flux results in a horizontal line, which means that the fluorescence inside (intact) vesicles remains constant, independent of fluorophore released from the empty vesicles. Graded flux results in a rising curve, because fluorescence increases as the quencher is released from the vesicles.
Data from Gregory et al. [16,17] and Clark et al. [26]. Left, replotted with permission from [16], Biophys. J. 94, 11044–11056 and Gregory et al. [17] 96, 116–131. Copyright (2008, 2009) by Elsevier. Right, replotted with permission from Clark et al. [26], Biochemistry 50, 7919–7932. Copyright (2011) American Chemical Society.

reliable means to assess translocation. But then, does it mean anything? We will also see that we require a direct measurement of translocation. Those issues will be discussed in light of recent experiments and calculations.

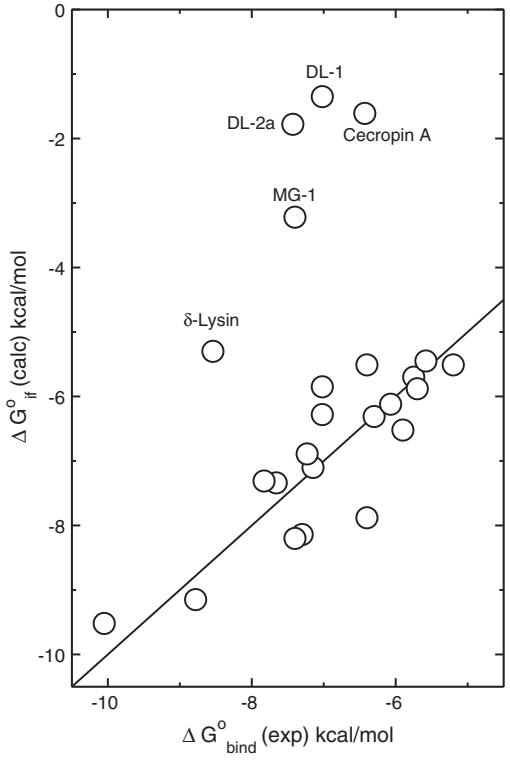

Fig. 3. Comparison of the Gibbs energy of peptide binding to a POPC membrane determined experimentally (ΔG^o_{bind}) with that calculated from the Wimley–White interfacial hydrophobicity scale (ΔG^o_{if}). The points correspond to the peptides listed in Table 1.

4. Peptide binding to the membrane interface

Let us consider first the binding step. Binding to POPC (or other PC membranes that are fluid at room temperature) can be calculated using the Wimley–White (WW) interfacial hydrophobicity scale for the amino acid residues [13,15] supplemented by end-group modifications (free N- and C-termini, N-terminal acetylation, C-terminal amidation) [30]. The software Membrane Protein Explorer (MPEx) provides a convenient way to perform these calculations [31,32]. For most peptides, the experimental Gibbs energy of binding (ΔG^o_{bind}) is remarkably well predicted by the ΔG^o_{if} calculated with the WW POPC interfacial scale (Table 1 and Fig. 3).

Fig. 3 shows experimental and calculated binding data for 24 membrane-active peptides. Of those 24 peptides, 19 show good agreement between the values calculated with the WW interfacial scale and obtained experimentally in different laboratories by different methods. The data points fall near the line with slope 1 and intercept 0. The outliers are mostly those noted above: δ-lysin and some of its variants (DL-1, DL-2a), cecropin A, and a variant of magainin 2 (MG-1).

The calculation of the Gibbs energy of binding to the membrane interface requires some caution [33]. If the peptide in solution is nearly completely unfolded (unstructured), and the content of α-helix (or other secondary structures) on the membrane is known, the process is straightforward. To calculate ΔG^o_{if}, one simply adds the hydrophobicities (more exactly, the Gibbs energies of transfer from water to a POPC bilayer interface) of all residues, the contributions of end groups, and the stabilization arising from helix formation at the interface. The latter amounts to $\Delta G^o_{res} \approx -0.4$ kcal/mol of hydrogen-bonded residues [34]. Several aspects are worth noting. First, if the peptide has some helical content (or other secondary structures) in water this needs to be taken into account, although the assumption that it is fully unfolded results only in a small error in ΔG^o_{if} [33]. Second, the contribution of −0.4 kcal/mol per helical residue arises from the additional stability of hydrogen bonds formed at the membrane interface, not from the amphipathicity (hydrophobic moment, μ_H) of the peptide [33]. Third, the process is purely additive, with no influence of sequence, but only of composition. Let us consider each of these aspects in more detail.

4.1. Helix formation in solution renders binding less favorable

The binding of a peptide to a membrane can be understood by the diagram of Fig. 4. The most convenient reference state for the calculation is the completely unfolded peptide conformation in water, because binding of unstructured peptides is what can be directly calculated with the Wimley–White (WW) interfacial scale. However, this is not the state that actually exists in solution. Rather, there is an ensemble of conformations, from unstructured to helical, with a mean helicity that can be determined experimentally by circular dichroism (CD) or NMR. The important point is that the Gibbs energy of the peptide ensemble in aqueous solution is lower than that of the unstructured state alone because additional (helical) conformations are available. Therefore, ΔG^o_{bind} measured experimentally, which is the difference between the Gibbs energy of the solution ensemble and the membrane-bound peptide, is lower in absolute value (less favorable) than it would be from the unstructured peptide in water (right side of Fig. 4).

It is easy to take the solution ensemble into account if the two-state approximation is made: the peptide is either folded or unfolded, and the measured helicity is an average, weighted by the populations of the two states. In that case, the partition function for the peptide in solution is simply $Q = 1 + K_\alpha$, where $K_\alpha = f_\alpha/(1 - f_\alpha)$, and f_α is the fraction of helical peptide in water, which is the measured helical content [33]. The Gibbs energy change for going from the fully unfolded reference state to the ensemble of helical and unfolded conformations (Fig. 4) is then $\Delta G^o_{helix,w} = -RT \ln(1 + K_\alpha)$. This effect is taken into account in the data shown in Table 1 and Fig. 3.

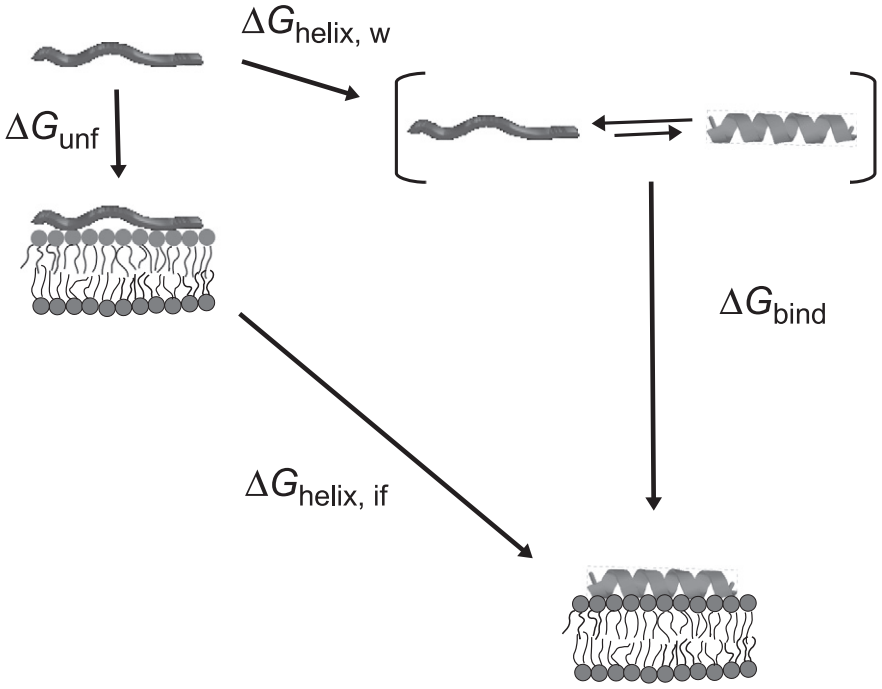

Fig. 4. Thermodynamic cycle connecting peptide folding in solution and on the membrane, and binding to the membrane. This figure expands the folding step in water, abbreviated in Fig. 1 by ΔG_f. The Gibbs free energies for each step are: ΔG_{unf}, binding of the fully unfolded state to the bilayer interface; ΔG_{bind}, Gibbs energy of binding from the actual aqueous solution ensemble to the bilayer interface; $\Delta G_{helix,w}$, Gibbs energy change in folding to produce the equilibrium ensemble from the unfolded state; and $\Delta G_{helix,if}$, Gibbs energy of folding the peptide, to the degree of helicity observed, in the membrane interface.

An important conclusion of this calculation is that, because the Gibbs energy of the aqueous state is lowered by helix formation, the Gibbs energy gap between the solution state and the bound state is reduced. As a consequence, peptides that have similar helical contents on the membrane but that are more helical in water bind worse to membranes, not better. As we will see below, it is the difference between the helical content on the membrane and in water that determines the contribution of secondary structure formation to binding. A second important aspect is that failure to take the solution ensemble into account can lead to erroneous conclusions regarding binding [33]. On the membrane, the measured helicity seems to correspond to a very narrow distribution about the mean helical content of the folded peptide, not to an ensemble that includes the unfolded state. That is, on the membrane, the peptide exists in a well-defined conformation with a helical content close to the experimental observable. The evidence comes from NMR structural data on magainin 2 [35], mastoparan X [36], and mastoparan [37,38], which shows no indication of unfolding on the membrane. Yet perhaps the most convincing evidence comes from recent MD simulations of melittin [39], which indicate a narrow distribution of helical states centered on a mean value (~78%) that is in good agreement with that measured experimentally (~70%).

4.2. Hydrogen bonds at the interface drive binding

As pointed out by Wimley et al. [28], the binding of the unstructured peptide to the membrane interface is almost always very weak, in fact undetectable for most practical purposes. What makes membrane-active peptides bind is the acquisition of secondary structure upon interaction with the membrane interface. This is called binding–folding coupling [13,15,28,34]: if the peptides bind they form α-helices (or β-

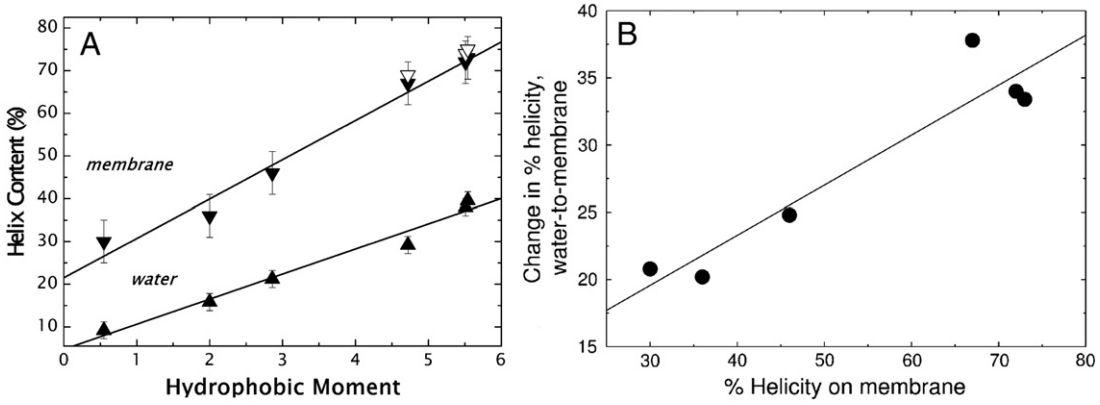

Fig. 5. (A) Correlation of the percent helicity with the hydrophobic moment (calculated for a full helix), in water and bound to a POPC membrane, for the AQL peptide family (see Table 1, AQL peptides are 17-residue, neutral peptides, with the formula: ac-$Ala_8Gln_3Leu_4$GW-amide). Solid symbols, the AQL peptides. Open symbols, the 26-residue melittin and the 31-residue peptide TMX-3 are included for comparison. (B) The same data for the AQL peptides, plotted as the increment in % helical content upon binding to the membrane as a function of the helicity on the membrane.
Panel A: Courtesy of Prof. Stephen White, UC Irvine. Reprinted with permission from Fernandez-Vidal et al. [40], J. Mol. Biol. 370, 459–470. Copyright (2007) Elsevier.

strand); if they desorb they unfold (for the most part). The question arises, however, of whether the extra stability that drives helix formation on the membrane is due to formation of intramolecular hydrogen bonds in the lower dielectric of the membrane interface (compared to water), or to the amphipathicity of the peptide, which allows it to segregate polar and hydrophobic residues, the former facing water, the latter, the membrane.

This problem was investigated in the AQL series of peptides (Table 1), in which the composition was maintained but the sequence was changed as a means to change the amphipathicity, quantitatively measured by the hydrophobic moment, μ_H [33,40]. The original calculation [40], however, did not correctly incorporate the effect of folding in water. When the existence of an ensemble of helical and unfolded conformations in solution is taken into account, it becomes clear that μ_H does not contribute to the Gibbs energy of helix formation at the membrane interface to any significant extent [33]. The incremental Gibbs energy due to helix formation per residue (ΔG^o_{res}) is constant, independent of peptide amphipathicity and sequence. Even for very different peptides, such as the AQL and the TP10 peptides, the same value of $\Delta G^o_{res} \approx -0.4$ kcal/mol per residue is obtained, as originally suggested by Ladokhin and White [34]. Thus, more favorable hydrogen bond formation by backbone peptide groups at the interface is what drives helix formation and consequent binding.

4.3. Amphipathicity enhances structure, not binding

This leaves us with a puzzling question: what is the role of amphipathicity in membrane-active peptides? The Wimley–White scale does not depend on sequence, and therefore on amphipathicity, yet it successfully predicts the correct binding for most peptides (Fig. 3). Most of the binding energy results from the establishment of hydrogen bonds upon helix formation on the membrane interface. Yet all naturally-occurring, α-helical membrane-active peptides are amphipathic. Why? The reason is that amphipathicity enhances helix formation. This is true not just on the membrane but also in water (Fig. 5A). The AQL peptides are monomeric in water [40], and their increase in helicity with hydrophobic moment is not a consequence of oligomerization, but an intrinsic property of the sequence. By increasing the tendency to adopt secondary structure, amphipathicity increases binding, because the formation of intramolecular hydrogen bonds in the membrane interface concomitant with the acquisition of secondary structure is the largest contributor to binding.

Thus, the propensity for α-helix formation on the membrane is driven by sequence in the same way as helix formation in water. Amphipathicity increases helicity in water because of interactions between nonpolar side chains spaced at positions i and $i+3$ or $i+4$ along the helix in the folded conformation [41–45]. These interactions are driven by the hydrophobic effect and van der Waals interactions between side chains of nonpolar residues [43]. Peptides that are more helical on the membrane are usually also more helical in water. Binding is improved by the increment in helicity on the membrane relative to water. This difference increases with the amphipathicity, which is measured by μ_H, resulting in the larger slope of the line corresponding to the membrane in Fig. 5A for the AQL peptides. Thus the increment in helicity upon binding to the membrane increases with the helical content of the peptides (Fig. 5B), which is why more helical peptides usually bind better. But that is in spite of their helical content in water, not because of it.

5. Translocation of peptides across the lipid bilayer

Consider now peptide translocation. The translocation of an amphipathic peptide across a membrane is by far less well understood than the binding step. First, charged molecules are not supposed to permeate lipid bilayers. Second, the initial state of the peptide, if and when it begins to cross the membrane, is not well characterized. Whether the peptides eventually form a pore, and independently of what their molecular

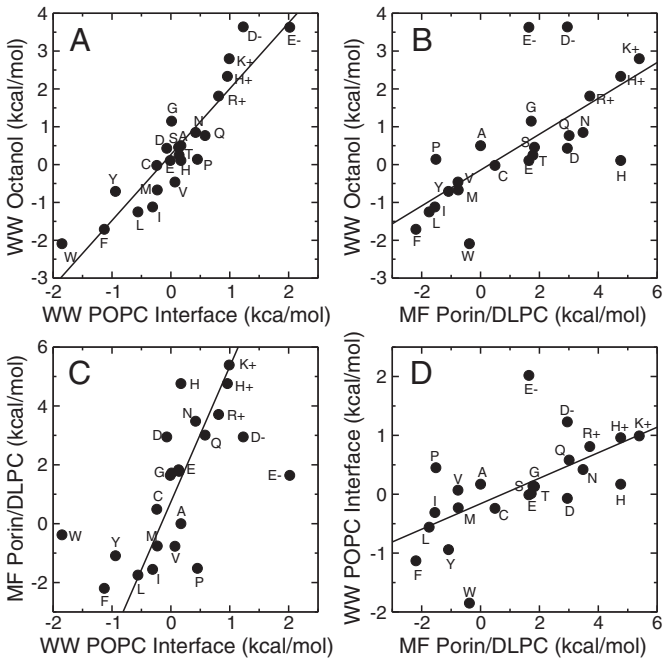

Fig. 6. Comparison of the most recent experimental hydrophobicity scales. The Gibbs energy of transfer of a peptide from an aqueous medium to a membrane-mimetic environment is compared among the Wimley–White (WW) scales (octanol and POPC interface) and the Moon–Fleming (MF) porin/DLPC scale. The plots in panels C and D are identical with the axes switched. It is duplicated because this allows easier comparison of each scale to the others. The slopes (m) and correlation coefficients (R) for each comparison are as follows: A, $m = 1.74$, $R = 0.92$; B, $m = 0.47$, $R = 0.71$; C, $m = 4.6$, $R = 0.61$; and D, $m = 0.217$, $R = 0.61$. The value for Ala was set to zero in the MF scale. Data for acidic and basic amino acids are given in the neutral and charged states. The MF scale determinations were made at pH 3.8.

organization may be in that pore, it seems reasonable that the initial stage of translocation will be determined by a free energy related to ΔG^o_{ins}. Since the peptide inserted in the membrane must be a high free energy state, its Gibbs energy is not accessible experimentally. Almeida and Pokorny [1] estimated it from $\Delta G^o_{ins} = \Delta G^o_{oct} - \Delta G^o_{bind}$ (Table 1). The values obtained are probably too large to represent peptide insertion, because ΔG^o_{oct} does not take into account bilayer reorganization, including redistribution and penetration of water molecules, which has been observed in MD simulations as the peptides sink deeper into the bilayer [7–11,46,47]. However, ΔG^o_{ins} should still provide an estimate of the relative ease that different peptides experience in inserting as monomers into the bilayer.

5.1. Hydrophobicity scales

The calculation of the Gibbs energies of binding and insertion made use of the WW scales for transfer of amino acid residues from water to the POPC interface or to octanol, as a mimic of the membrane interior. The values calculated for binding are in good agreement with direct experimental measurements for most peptides (Fig. 3). The values calculated for insertion, from $\Delta G^o_{ins} = \Delta G^o_{oct} - \Delta G^o_{bind}$, depend of course on the hydrophobicity scale used for the membrane interior. We have used the WW octanol hydrophobicity scale; the values would be different if a different scale were used. Does the choice of hydrophobicity scale significantly affect the predictions for binding and translocation? Let us briefly consider the effect of using other scales.

The WW POPC interfacial and octanol hydrophobicity scales are experimental, whole-residue scales. They measure the transfer of an amino acid residue (–NHCRHCO–) from water to a nonpolar environment. No other hydrophobicity scale exists for binding to the membrane interface. However, there are several scales available for transfer to the membrane interior. MacCallum and Tieleman [48] compared and

discussed several of these scales: Radzika–Wolfenden (RW) [49], Wimley–White (WW) octanol [12], MacCallum–Tieleman (MT) [50], and Moon–Fleming (MF) porin scale [51]. All scales are correlated [48]. The WW POPC interfacial scale was not included in the comparison, because it refers to transfer to the membrane interface whereas all other scales refer to transfer from water to the membrane interior or its mimics [48]. Therefore, the WW POPC scale is compared to the WW octanol and the MF scales in Fig. 6. We see that the interfacial scale, too, is correlated with the others. The slopes of the correlation plots are: WW octanol/WW interface, 1.74; MF/WW octanol, 2.1; and MF/WW interface, 4.6. Thus, there is a scale factor of ~2 in the hydrophobicity values going from WW interfacial to WW octanol to MF porin scale.

It should be noted that, except for the two WW scales, all others refer to the transfer of an amino acid side chain or its analog from water to a nonpolar medium. The peptide group is not included in any of them; its inclusion would make all the transfers to the membrane more unfavorable. The RW is an experimental scale for transfer of side chains to

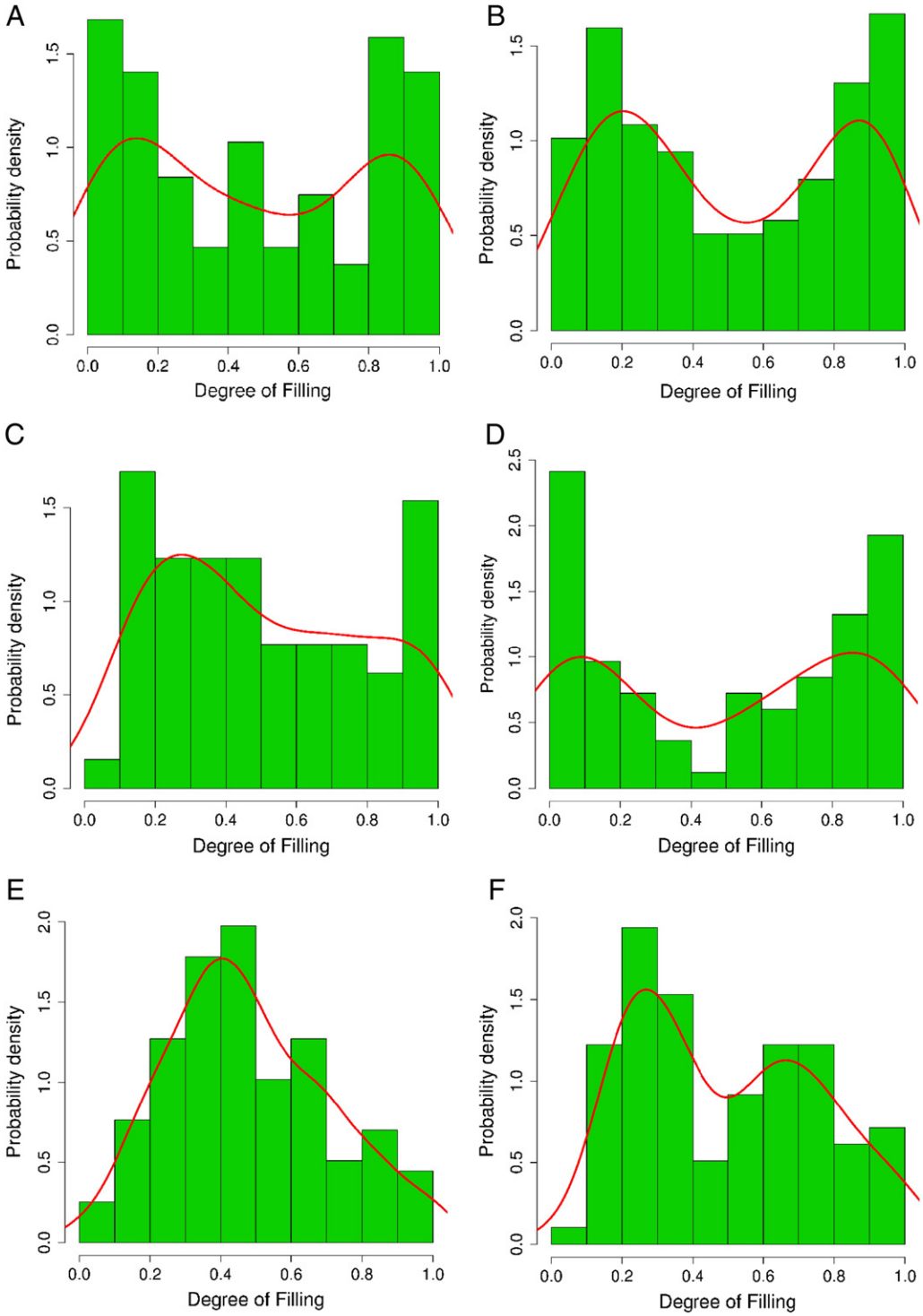

Fig. 7. Histograms (green) and probability density functions (red) of the distributions of degree of filling of POPC GUVs, at the influx midpoint, with the peptides: (A) CE-2, (B) DL-1, (C) δ-lysin, (D) TPW-3, (E) CE-2, and (F) TPW-3. A–D, GUVs with $d > 15$ μm, E–F, GUVs with $d < 15$ μm.
Reprinted with permission from Wheaten et al. [52], Biophys. J. 105, 432–443. Copyright (2013) Elsevier.

hexane. The MT scale is theoretical, derived from MD simulations, and compares side chain transfers from water to the bilayer interior.

The MF scale is the newest one, and is especially interesting because it is experimental and the nonpolar medium is a bilayer (dilauroylphosphatidylcholine, DLPC). It compares the Gibbs energies of other amino acid side chains inside the DLPC bilayer with that of Ala (which is set to zero in Fig. 6) at a specific position (residue 210) in the middle of an integral membrane protein, the β-barrel porin OmpLA. Setting $\Delta G^o = 0$ for transfer of Ala to the membrane places this residue at about the same level it occupies in the WW octanol and interfacial scales, where $\Delta G^o_{if} = 0.17$ and $\Delta G^o_{oct} = 0.50$ kcal/mol for Ala. In Fig. 6, the correlation between the MF and WW octanol scales is excellent except for Trp, the negatively charged Asp and Glu, and the neutral His, which clearly fall off the line. However, the values in the octanol scale for neutral Asp and Glu, and cationic His, match those in the MF scale. This is because the pH was 3.8 in the experiments used to establish the MF scale, so that Asp and Glu were neutral, and His was cationic in the porin.

In conclusion, the values of ΔG^o_{ins} depend quantitatively on the scale, but the trend does not. Thus a if a threshold exists, which separates peptides that are able translocate—because ΔG^o_{ins} is sufficiently small—from those that are not, it will be found with any scale.

5.2. The meaning of graded and all-or-none release

We had noticed that some peptides did not obey the trend that graded release corresponds to $\Delta G^o_{ins} \leq 20$ kcal/mol, and all-or-none, to $\Delta G^o_{ins} > 23$ kcal/mol. CE-2 and MG-2 are examples, and without assuming side-chain salt bridges, δ-lysin is too. But we decided to test the idea further. If the type of induced release is a property of the peptide, it should not depend on the vesicle type. In the case of magainin 2, for example, the release is all-or-none in both LUVs and GUVs. But not many peptides have been examined in both kinds of lipid vesicles for the type of release they induce.

Wheaten et al. [52] tested the idea in four additional peptides, CE-2, δ-lysin, DL-1, and TPW-3, which had been previously studied in LUVs, by determining the release type in GUVs. Fig. 7 shows the distributions of dye content (or degree of filling) in GUVs, as histograms and density functions, at the midpoint of the influx induced by those four peptides. Unimodal distributions correspond to graded flux—most vesicles behave similarly to the average—and bimodal distributions correspond to all-or-none flux—most vesicles are either full or empty [21,52,53]. CE-2 causes graded dye flux in LUVs and small GUVs (diameter, $d < 15$ μm, Fig. 7E) but causes all-or-none flux in large GUVs ($d > 15$ μm, Fig. 7A). Thus the type of flux can change with the type of vesicle. Further, the observation of graded flux in CE-2 is contrary to the idea that graded release corresponds to $\Delta G^o_{ins} \leq 20$ kcal/mol, as $\Delta G^o_{ins} = 36$ kcal/mol for CE-2. The result with TPW-3 also contradicts this idea because TPW-3 causes all-or-none flux in large GUVs (Fig. 7D) even though its $\Delta G^o_{ins} = 17$ kcal/mol. Thus, there are too many exceptions to the conjectured relation between a threshold in ΔG^o_{ins} and the observation graded or all-or-none flux. Whether the main hypothesis is correct regarding the relation between peptide translocation and a threshold in ΔG^o_{ins} cannot be assessed from these data.

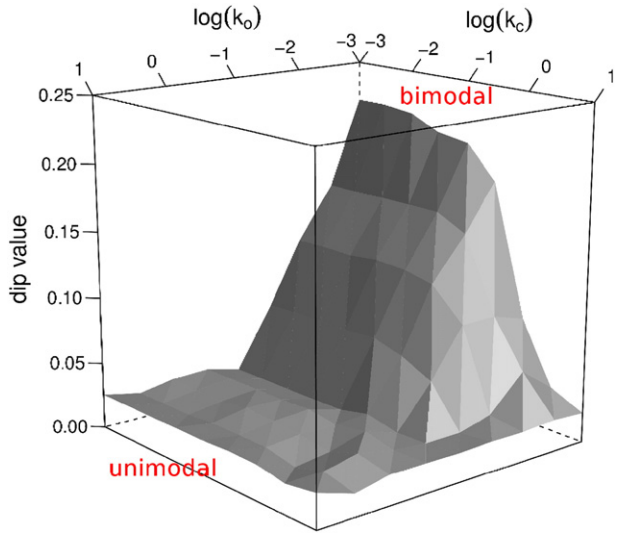

Fig. 8. Unimodal distribution (graded flux) and bimodal distribution (all-or-none flux) obtained in Monte Carlo simulations as a function of the rate constants for pore opening (k_o) and closing (k_c), in a logarithmic scale of base 10, with fixed flux rate constant $k_x = 1\ s^{-1}$. The dip statistic is plotted on the y-axis. Unimodal distributions (graded flux) appear at the base of the plot, whereas bimodal distributions (all-or-none flux) appear at the top.
Reprinted with permission from Wheaten et al. [52], Biophys. J. 105, 432–443. Copyright (2013) Elsevier.

The reason for the lack of correspondence between ΔG^o_{ins} and the type of flux can be understood from Monte Carlo simulations [52]. These simulations showed that graded flux can be obtained by several combinations of the relative magnitudes of the rate constants of pore opening (k_o), pore closing (k_c), and dye flux (k_x). Those rate constants determine the modality (uni- or bimodal) of dye content distributions. Hartigan's dip statistic is a measure of the probability that a distribution be unimodal [54]. Fig. 8 shows a surface plot of the value of Hartigan's dip statistic test for modality as a function of k_o and k_c at constant $k_x = 1\ s^{-1}$. The dip statistic is large for bimodal distributions (all-or-none flux), which correspond to the top of the surface, and approaches zero for unimodal distributions (graded flux), which correspond to the base of the surface. All-or-none flux results when both k_o and k_c are much smaller than k_x. However, graded flux can occur by increasing k_c, which had long been shown by Schwarz [55], but also by increasing k_o, keeping the other processes slow compared with the dye flux. All-or-none flux requires long-lived pores (in comparison with the flux time) but it is also possible to obtain graded flux with long-lived pores: the flux just becomes faster. Thus, there are multiple mechanistic ways to obtain graded flux, which may be different for different peptides. In essence, the graded and all-or-none nature of the fluxes, as assessed experimentally, is statistical: it reflects the distribution of the dye content in the vesicles [52]. But from a knowledge of the type of flux caused by a given peptide, it is difficult to derive kinetic or mechanistic information, or to infer the ability of the peptide to translocate across the bilayer.

MD simulations have revealed pore characteristics that generally match the ideas proposed based on dye flux experiments [9–11,46]. For example, in simulations, magainin 2 forms large pores whereas melittin forms small transient pores. This is consistent with the all-or-none flux induced by magainin and the graded flux induced by melittin. But both peptides are able to translocate across the bilayer in the MD simulations. This is consistent with the lack of a direct relation between translocation and the type of flux.

5.3. Peptide translocation

Direct assessment of peptide translocation is therefore necessary if the original hypothesis is to be tested. This has been a particularly difficult experimental problem. Several methods proposed earlier are prone to artifacts [56–58]. Recently, however, new methods were developed that allow for an unambiguous answer to the question of whether a peptide translocates across a lipid bilayer [2,3]. The latest was developed in our laboratory [4]. It makes use of very large GUVs, with $d \approx 100$ μm, that contain smaller ones, with $d \approx 10$–20 μm, inside (Fig. 9). When these GUVs with inner vesicles are placed in a solution containing the peptide and a water-soluble dye they appear initially black. As the peptide interacts with the outer membrane and causes dye to enter the larger GUV, the vesicle lumen begins to fluoresce. But the inner GUVs remain dark unless the peptide crosses the outer membrane and interacts with the inner membranes. If that happens, the lumen of the inner vesicles also becomes

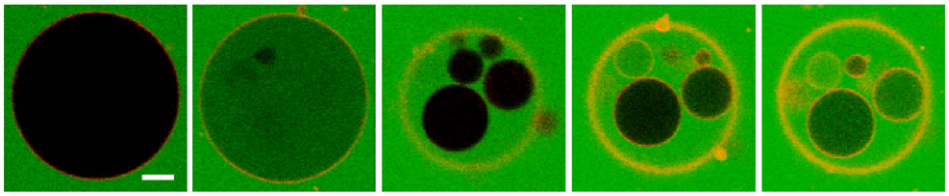

Fig. 9. Time sequence of carboxyfluorescein (CF) influx (green fluorescence) into POPC GUVs, after addition to a solution of the peptide TP10W labeled with rhodamine lissamine on the N-terminus (Rh-TP10W). The rhodamine channel (red) is slightly enhanced to improve visibility of the peptide on the membrane. Times, from left to right: 8.5, 14, 33, 60, and 75 min. Scale bar, 10 μm.
Reprinted with permission from Wheaten et al. [4], J. Am. Chem. Soc. 135, 16517–16525. Copyright (2013) American Chemical Society.

fluorescent. If the peptide is covalently labeled with another fluorophore its entry can be visualized directly by the appearance of peptide fluorescence on the inner membranes [4]. Using this method, Wheaten et al. [4] showed that rhodamine-labeled TP10W (Rh-TP10W), for which $\Delta G^o_{ins} \approx 17$ kcal/mol, readily translocates across pure lipid bilayers. Rh-DL-1-amide ($\Delta G^o_{ins} \approx 24$ kcal/mol) also translocates, but less efficiently; and CE-2 ($\Delta G^o_{ins} = 35$ kcal/mol) shows very little translocation. Thus a correlation appears to exist between ΔG^o_{ins} and the ability to translocate. This agrees with the main hypothesis, but the dependence of translocation on ΔG^o_{ins} is continuous, not a sharp threshold.

Wheaten et al. [4] also measured the kinetics of translocation of fluorescently labeled peptides by the rate of peptide accumulation on the membranes of the inner vesicles. Fig. 10A shows a large GUV, containing five smaller vesicles inside with $d \approx 10$ μm (scale bar). In this image, the outer vesicle has already allowed complete dye influx. The inner vesicle on the lower right corner of Fig. 10A has undergone about 50% influx. Fig. 10C shows the kinetics of dye influx (green symbols). The accumulation of peptide on the membrane of this inner vesicle occurs in a time of ~10 min (red symbols). This accumulation reflects the rate-limiting process, which is translocation across the membrane of the outer GUV. Peptide binding and dissociation from the bilayer occur much faster, in a timescale of <1 s [4].

These results show that peptide translocation is not coupled with dye flux. Translocation of the peptide Rh-TP10W across the membrane of a GUV occurs mainly after the dye flux into that vesicle has occurred [4]. This was surprising and contrary to the assumption used in the analysis of dye efflux kinetics in LUVs [6,18–20]. A possible explanation is suggested based on recent MD simulations [46]. In MD simulations, the free energy barrier for reorientation of the peptide melittin, from a position parallel to the membrane surface to a transmembrane orientation, is reduced if another melittin molecule is already inserted in the membrane [46]. The largest free energy barrier arises in the insertion of the first peptide. In all the cases where we have experimentally examined the kinetics of peptide-induced dye efflux in LUVs, those kinetics were found to be consistent with the insertion of monomers, perhaps dimers, but not with oligomers larger than trimers (and a trimer was only consistent with the kinetics in the case of δ-lysin) [6,16–20]. However, if insertion of the first few peptides causes most of the dye flux, then the efflux kinetics in LUVs will not reflect translocation, which would happen mainly after efflux occurred [4]. Consequently, any cooperative interactions between peptides that may occur during translocation would go undetected in the dye efflux experiments in LUVs.

6. Summary

We proposed the hypothesis that peptide translocation across a membrane is determined by its Gibbs energy of insertion (ΔG^o_{ins}) into the bilayer [1]. Based on peptide-induced dye-flux experiments, we further suggested that a threshold exists: for translocation to occur $\Delta G^o_{ins} \leq 20$ kcal/mol. Finally, we conjectured that translocation and the type of dye flux, graded or all-or-none, were related. Graded dye flux would occur concomitant with peptide translocation, which would explain incomplete dye release, whereas all-or-none flux would occur with peptides that cannot translocate, because $\Delta G^o_{ins} > 23$ kcal/mol, and therefore these accumulate on the membrane until a rupture point is reached that results in complete dye release.

The central role played by ΔG^o_{ins} in the main hypothesis requires a careful consideration of the two terms that compose it. $\Delta G^o_{ins} = \Delta G^o_{oct} - \Delta G^o_{bind}$, where ΔG^o_{oct} is the Gibbs energy of transfer from water to the bilayer interior, calculated using the WW scale for transfer to octanol, and ΔG^o_{bind} is the Gibbs energy of binding from water to the membrane surface. We found that ΔG^o_{bind} is well understood, and with rare exceptions can be well approximated by ΔG^o_{if} calculated with the WW interfacial hydrophobicity scale. ΔG^o_{oct} may not accurately represent peptide transfer to the bilayer interior, but all hydrophobicity scales are correlated; thus an equivalent threshold would always be found for ΔG^o_{ins}, even if with a value ≠ 20 kcal/mol.

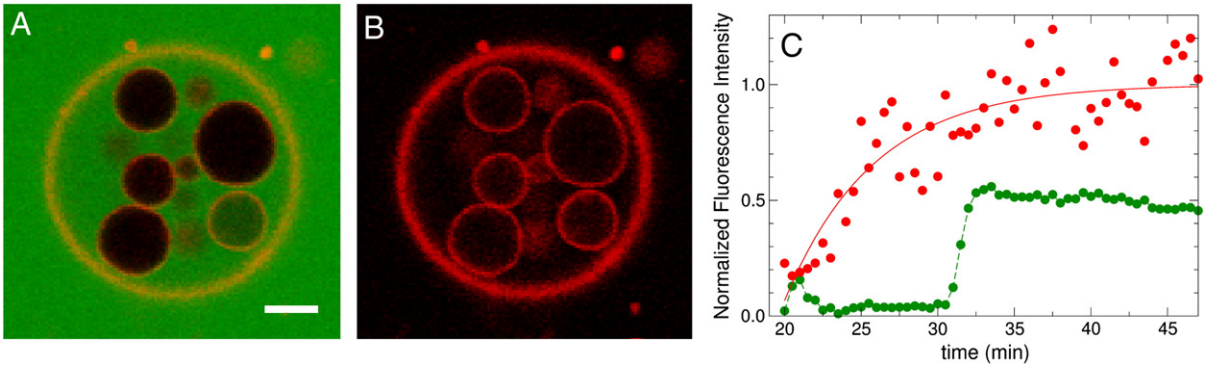

Fig. 10. A large GUV containing several inner vesicles after addition of the fluorescently labeled peptide Rh-TP10W. (A) Carboxyfluorescein (external aqueous dye) and rhodamine (peptide label) channels. Scale bar, 10 μm. (B) Same GUV, rhodamine channel only, contrast enhanced. (C) Kinetics of dye influx and peptide translocation. The red data points show the Rh-TP10W fluorescence from the membrane of the inner vesicle seen at the bottom right in panel (A), as a function of time. The red line is a fit of an exponential rising function to the data. The green data points show the carboxyfluorescein channel, corresponding to flux into the lumen of the same inner vesicle. The green line is to guide the eye. The images in (A) and (B) are taken 44 min after addition to the peptide solution, toward the end of the time trace shown in (C).
Reprinted with permission from Wheaten et al. [4], J. Am. Chem. Soc. 135, 16517–16525. Copyright (2013) American Chemical Society.

If those ideas were correct, translocation and the type of dye flux should not depend on sequence but only on ΔG^o_{ins}. However, we found that conservative sequence changes that do not affect ΔG^o_{ins} can change dye release from all-or-none to graded. The idea that the type of release is related to peptide translocation was then questioned. On further testing, we found that the hypothesis that translocation occurs if $\Delta G^o_{ins} \leq 20$ kcal/mol may be correct, but the conjectured relation to graded or all-or-none flux is not. Whereas graded and all-or-none fluxes may provide hints about the peptide mechanism, even consistent with MD simulations, they are not conclusive regarding peptide translocation.

Finally, having developed a new method, we directly determined peptide translocation in GUVs. We found that translocation occurred for all peptides examined; however, in agreement with the main hypothesis, it appears to be more likely the smaller the ΔG^o_{ins} of the peptide. How generally valid this conclusion may be, however, remains to be seen. Provided with this method, we were also able to measure peptide translocation and dye flux in the same GUV. To our surprise, we found that peptide translocation and dye flux across the membrane are not concomitant: they are not mechanistically coupled. Even though they occur broadly over the same time period, their detailed kinetics are different. Thus, these two processes are both consequences of the same peptide-induced perturbation of the membrane, but there seems to be no causal relation between them.

Acknowledgment

This work was supported by grant GM072507 from the National Institutes of Health.

References

[1] P.F. Almeida, A. Pokorny, Mechanism of antimicrobial, cytolytic, and cell-penetrating peptides: from kinetics to thermodynamics, Biochemistry 48 (2009) 8083–8093.
[2] J.R. Marks, J. Placone, K. Hristova, W.C. Wimley, Spontaneous membrane-translocating peptides by orthogonal high-throughput screening, J. Am. Chem. Soc. 133 (2011) 8995–9004.
[3] J. He, K. Hristova, W.C. Wimley, A highly charged voltage-sensor helix spontaneously translocates across membranes, Angew. Chem. Int. Ed. 51 (2012) 7150–7153.
[4] S.A. Wheaten, F.D.O. Ablan, B.L. Spaller, J.M. Trieu, P.F. Almeida, Translocation of cationic amphipathic peptides across the membranes of pure phospholipid giant vesicles, J. Am. Chem. Soc. 135 (2013) 16517–16525.
[5] G.S. Hammond, A correlation of reaction rates, J. Am. Chem. Soc. 77 (1955) 334–338.
[6] L.E. Yandek, A. Pokorny, A. Floren, K. Knoelke, U. Langel, P.F.F. Almeida, Mechanism of the cell-penetrating peptide Tp10 permeation of lipid bilayers, Biophys. J. 92 (2007) 2434–2444.
[7] H. Leontiadou, A.E. Mark, S.J. Marrink, Antimicrobial peptides in action, J. Am. Chem. Soc. 128 (2006) 12156–12161.
[8] D. Sengupta, H. Leontiadou, A.E. Mark, S.J. Marrink, Toroidal pores formed by antimicrobial peptides show significant disorder, Biochim. Biophys. Acta 1778 (2008) 2308–2317.
[9] S.J. Irudayam, M.L. Berkowitz, Binding and reorientation of melittin in a POPC bilayer: computer simulations, Biochim. Biophys. Acta 1818 (2012) 2975–2981.
[10] K.P. Santo, M.L. Berkowitz, Difference between magainin-2 and melittin assemblies in phosphatidylcholine bilayers: results from coarse-grained simulations, J. Phys. Chem. B 116 (2012) 3021–3030.
[11] K.P. Santo, S.J. Irudayam, M.L. Berkowitz, Melittin creates transient pores in a lipid bilayer: results from computer simulations, J. Phys. Chem. B 117 (2013) 5031–5042.
[12] W.C. Wimley, T.P. Creamer, S.H. White, Solvation energies of amino acid side chains and backbone in a family of host/guest pentapeptides, Biochemistry 35 (1996) 5109–5124.
[13] S.H. White, W.C. Wimley, Membrane protein folding and stability: physical principles, Annu. Rev. Biophys. Biomol. Struct. 28 (1999) 319–365.
[14] S. Jayasinghe, K. Hristova, S.H. White, Energetics, stability, and prediction of transmembrane helices, J. Mol. Biol. 312 (2001) 927–934.
[15] W.C. Wimley, S.H. White, Experimentally determined hydrophobicity scale of proteins at membrane interfaces, Nat. Struct. Biol. 3 (1996) 842–848.
[16] S.M. Gregory, A.C. Cavenaugh, V. Journigan, A. Pokorny, P.F.F. Almeida, A quantitative model for the all-or-none permeabilization of phospholipid vesicles by the antimicrobial peptide cecropin A, Biophys. J. 94 (2008) 1667–1680.
[17] S.M. Gregory, A. Pokorny, P.F.F. Almeida, Magainin 2 revisited: a test of the quantitative model for the all-or-none permeabilization of phospholipid vesicles, Biophys. J. 96 (2009) (2009) 116–131.
[18] A. Pokorny, T.H. Birkbeck, P.F.F. Almeida, Mechanism and kinetics of δ-lysin interaction with phospholipid vesicles, Biochemistry 41 (2002) 11044–11056.
[19] A. Pokorny, P.F.F. Almeida, Kinetics of dye efflux and lipid flip-flop induced by δ-lysin in phosphatidylcholine vesicles and the mechanism of graded release by amphipathic, α-helical peptides, Biochemistry 43 (2004) 8846–8857.
[20] L.E. Yandek, A. Pokorny, P.F.F. Almeida, Wasp mastoparans follow the same mechanism as the cell-penetrating peptide transportan 10, Biochemistry 48 (2009) 7342–7351.
[21] P.F. Almeida, Pokorny, Interactions of antimicrobial peptides with lipid bilayers, in: Edward H. Egelman (Ed.), Comprehensive Biophysics, Membranes, Lukas TammAcademic Press, Oxford, 2012, pp. 189–222.
[22] W.C. Wimley, M.E. Selsted, S.H. White, Interactions between human defensins and lipid bilayers: evidence for formation of multimeric pores, Protein Sci. 3 (1994) 1362–1373.
[23] A.S. Ladokhin, W.C. Wimley, S.H. White, Leakage of membrane vesicle contents: determination of mechanism using fluorescence requenching, Biophys. J. 69 (1995) 1964–1971.
[24] A.S. Ladokhin, W.C. Wimley, K. Hristova, S.H. White, Mechanism of leakage of contents of membrane vesicles determined by fluorescence requenching, Methods Enzymol. 278 (1997) 474–486.
[25] A.N. McKeown, J.L. Naro, L.J. Huskins, P.F. Almeida, A thermodynamic approach to the mechanism of cell-penetrating peptides in model membranes, Biochemistry 50 (2011) 654–662.
[26] K.S. Clark, J.A. Svetlovics, A.N. McKeown, L.J. Huskins, P.F. Almeida, What determines the activity of antimicrobial and cytolytic peptides in model membranes, Biochemistry 50 (2011) 7919–7932.
[27] Y. Tamba, M. Yamazaki, Single giant unilamellar vesicle method reveals effect of antimicrobial peptide magainin 2 on membrane permeability, Biochemistry 44 (2005) 15823–15833.
[28] W.C. Wimley, K. Hristova, A.S. Ladokhin, L. Silvestro, P.H. Axelsen, S.H. White, Folding of β-sheet membrane proteins: a hydrophobic hexapeptide model, J. Mol. Biol. 277 (1998) 1091–1110.
[29] W.C. Wimley, K. Gawrisch, T.P. Creamer, S.H. White, Direct measurement of salt-bridge solvation energies using a peptide model system: implications for protein stability, Proc. Natl. Acad. Sci. U. S. A. 93 (1996) 2985–2990.
[30] K. Hristova, S.H. White, An experiment-based algorithm for predicting the partitioning of unfolded peptides into phosphatidylcholine bilayer interfaces, Biochemistry 44 (2005) 12614–12619.
[31] C. Snider, S. Jayasinghe, K. Hristova, S.H. White, MPEx: a tool for exploring membrane proteins, Protein Sci. 18 (2009) 2624–2628.
[32] S. Jayasinghe, K. Hristova, W. Wimley, C. Snider, S.H. White, Membrane Protein Explorer, 2013. (http://blanco.biomol.uci.edu/MPEx).
[33] P.F. Almeida, A.S. Ladokhin, S.H. White, Hydrogen-bond energetics drive helix formation in membrane interfaces, Biochim. Biophys. Acta 1818 (2012) 178–182.
[34] A.S. Ladokhin, S.H. White, Folding of amphipathic α-helices on membranes: energetics of helix formation by melittin, J. Mol. Biol. 285 (1999) 1363–1369.
[35] J. Gesell, M. Zasloff, S.J. Opella, Two-dimensional ^{1}H-NMR experiments show that the 23-residue magainin antibiotic peptide is an α-helix in dodecylphosphocholine micelles, sodium dodecylsulfate micelles, and trifluoroethanol/water solution, J. Biomol. NMR 9 (1997) 127–135.
[36] Y. Todokoro, I. Yumen, K. Fukushima, S.-W. Kang, J.-S. Park, T. Kohno, K. Wakamatsu, H. Akutsu, T. Fujiwara, Structure of tightly membrane-bound mastoparan-X, a G-protein-activating peptide, determined by solid-state NMR, Biophys. J. 91 (2006) 1368–1379.
[37] R.R. Vold, R.S. Prosser, A.J. Deese, Isotropic solutions of phospholipid bicelles: a new membrane mimetic for high-resolution NMR studies of polypeptides, J. Biomol. NMR (1997) 329–335.
[38] Y. Hori, M. Demura, M. Iwadate, A.S. Ulrich, T. Niidome, H. Aoyagi, T. Asakura, Interaction of mastoparan with membranes studied by ^{1}H-NMR spectroscopy in detergent micelles and by solid-state ^{2}H-NMR and ^{15}N-NMR spectroscopy in oriented lipid bilayers, Eur. J. Biochem. 268 (2001) 302–309.
[39] M. Andersson, J.P. Ulmschneider, M.B. Ulmschneider, S.H. White, Conformational states of melittin at a bilayer interface, Biophys. J. 104 (2013) L12–L14.
[40] M. Fernandez-Vidal, S. Jayasinghe, A.S. Ladokhin, S.H. White, Folding amphipathic helices into membranes: amphiphilicity trumps hydrophobicity, J. Mol. Biol. 370 (2007) 459–470.
[41] S. Padmanabhan, R.L. Baldwin, Tests for helix-stabilizing interactions between various nonpolar side chains in alanine-based peptides, Protein Sci. 3 (1994) 1992–1997.
[42] S. Padmanabhan, R.L. Baldwin, Helix-stabilizing interaction between tyrosine and leucine or valine when the spacing is $i,i+4$, J. Mol. Biol. 241 (1994) 706–713.
[43] T.P. Creamer, G.D. Rose, Interactions between hydrophobic side chains within α-helices, Protein Sci. 4 (1995) 1305–1314.
[44] H. Xiong, B.L. Buckwalter, H.-M. Shieh, M.H. Hecht, Periodicity of polar and nonpolar amino acids is the major determinant of secondary structure in self-assembling oligomeric peptides, Proc. Natl. Acad. Sci. U. S. A. 9 (1995) 6349–6353.
[45] A. Chakrabartty, R.L. Baldwin, Stability of α-helices, Adv. Protein Chem. 46 (1995) 141–176.
[46] S.J. Irudayam, T. Pobandt, M.L. Berkowitz, Free energy barrier for melittin reorientation from a membrane-bound state to a transmembrane state, J. Phys. Chem. B 117 (2013) 13457–13463.
[47] C.M. Dunkin, A. Pokorny, P.F. Almeida, H.-S. Lee, Molecular dynamics studies of transportan 10 (Tp10) interacting with a POPC lipid bilayer, J. Phys. Chem. B 115 (2011) 1188–1198.
[48] J.L. MacCallum, D.P. Tieleman, Hydrophobicity scales: a thermodynamic looking glass into lipid–protein interactions, Trends Biochem. Sci. 36 (2011) 653–662.
[49] A. Radzicka, R. Wolfenden, Comparing the polarities of the amino acids: side-chain distribution coefficients between the vapor phase, cyclohexane, 1-octanol, and neutral aqueous-solution, Biochemistry 27 (1988) 1664–1670.
[50] J.L. MacCallum, D.P. Tieleman, Distribution of amino acids in a lipid bilayer from computer simulations, Biophys. J. 94 (2008) 3393–3404.
[51] C.P. Moon, K.G. Fleming, Side chain hydrophobicity scale derived from transmembrane protein folding into lipid bilayers, Proc. Natl. Acad. Sci. U. S. A. 108 (2011) 10174–10177.

[52] S.A. Wheaten, A. Lakshmanan, P.F. Almeida, Statistical analysis of peptide-induced graded and all-or-none fluxes in giant vesicles, Biophys. J. 105 (2013) 432–443.
[53] B. Apellániz, J.L. Nieva, P. Schwille, A.J. García-Sáez, All-or-none versus graded: single-vesicle analysis reveals lipid composition effects on membrane permeabilization, Biophys. J. 99 (2010) 3619–3628.
[54] J.A. Hartigan, P.M. Hartigan, The dip test of unimodality, Ann. Stat. 13 (1985) 70–84.
[55] G. Schwarz, C.H. Robert, Kinetics of pore-mediated release of marker molecules from liposomes or cells, Biophys. Chem. 42 (1992) 291–296.
[56] K. Matsuzaki, O. Murase, N. Fujii, K. Miyaijima, Translocation of a channel-forming antimicrobial peptide, magainin 2, across lipid bilayers by forming a pore, Biochemistry 34 (1995) 6521–6526.
[57] K. Matsuzaki, S. Yoneyama, O. Murase, K. Miyaijima, Transbilayer transport of ions and lipids coupled with mastoparan X translocation, Biochemistry 35 (1996) 8450–8456.
[58] S. Kobayashi, A. Chikushi, S. Tougu, Y. Imura, M. Nishida, Y. Yano, K. Matsuzaki, Translocation of a channel-forming antimicrobial peptide, magainin 2, across lipid bilayers by forming a pore, Biochemistry 43 (2004) 15610–15616.
[59] AGADIR, an algorithm to predict the helical content of peptides is available on-line at http://agadir.crg.es/, 2013.
[60] V. Muñoz, L. Serrano, Elucidating the folding problem of helical peptides using empirical parameters, Nat. Struct. Biol. 1 (1994) 399–409.
[61] V. Muñoz, L. Serrano, Elucidating the folding problem of α-helical peptides using empirical parameters. II. Helix macrodipole effects and rational modification of the helical content of natural peptides, J. Mol. Biol. 245 (1994) 275–296.
[62] V. Muñoz, L. Serrano, Elucidating the folding problem of a-helical peptides using empirical parameters. III: Temperature and pH dependence, J. Mol. Biol. 245 (1994) 297–308.
[63] V. Muñoz, L. Serrano, Development of the multiple sequence approximation within the Agadir model of α-helix formation. Comparison with Zimm–Bragg and Lifson–Roig formalisms, Biopolymers 41 (1997) 495–509.
[64] E. Lacroix, A.R. Viguera, L. Serrano, Elucidating the folding problem of α-helices: local motifs, long-range electrostatics, ionic strength dependence and prediction of NMR parameters, J. Mol. Biol. 284 (1998) 173–191.
[65] L.E. Yandek, A. Pokorny, P.F.F. Almeida, Small changes in the primary structure of transportan 10 alter the thermodynamics and kinetics of its interaction with phospholipid vesicles, Biochemistry 47 (2008) 3051–3060.
[66] G. Klocek, T. Schulthess, Y. Shai, J. Seelig, Thermodynamics of melittin binding to lipid bilayers. Aggregation and pore formation, Biochemistry 48 (2009) 2586–2596.
[67] E. Kuchinka, J. Seelig, Interaction of melittin with phosphatidylcholine membranes. Binding isotherm and lipid head-group conformation, Biochemistry 28 (1989) 4216–4221.
[68] D. Allende, S.A. Simon, T.J. McIntosh, Melittin-induced bilayer leakage depends on lipid material properties: evidence for toroidal pores, Biophys. J. 88 (2005) 1828–1837.
[69] S.H. White, W.C. Wimley, A.S. Ladokhin, K. Hristova, Protein folding in membranes: determining energetics of peptide–bilayer interactions, Methods Enzymol. 295 (1998) 62–87.
[70] M.A. Cherry, S. Higgins, H. Melroy, H.-S. Lee, A. Pokorny, Peptides with the same composition, hydrophobicity, and hydrophobic moment bind to phospholipid bilayers with different affinities, 2014. (in preparation).